Soft Matter

Accepted Manuscript

This article can be cited before page numbers have been issued, to do this please use: H. Kim, D. Costa and J. Kim, *Soft Matter*, 2026, DOI: 10.1039/D6SM00297H.

ROYAL SOCIETY OF CHEMISTRY

rsc.li/soft-matter-journal

View Article Online
DOI: 10.1039/D6SM00297H

Viscous solvent embrittles long-chain polymer networks

Haeji Kim, Diogo Costa, Junsoo Kim*

Department of Mechanical Engineering, Northwestern University, Evanston, Illinois 60208, United States

*Junsoo Kim; Phone: +1 (847) 491-4322, e-mail: junsoo.kim@northwestern.edu

Abstract

The toughness of polymer networks is commonly attributed to energy dissipation arising from viscoelastic deformation, leading to a design principle: higher viscosity increases toughness. Here, we show that this relationship can be reversed when polymer chains are sufficiently long. To demonstrate, we prepare polyacrylamide hydrogels with identical network structures, fully dry them, and reswell them in glycerol-water mixtures to the same polymer content, thereby varying the solvent viscosity by three orders of magnitude while preserving the network structure. Although the mechanical response under homogeneous deformation does not change significantly, toughness measured by pure shear and trouser tests markedly decreases with solvent viscosity. In particular, toughness collapses onto a master curve when plotted as a function of the product of viscosity and velocity, with a scaling relation consistent with the shear-lag model. Stick-slip occurs under conditions for which the slope of the master curve is negative, corroborating the presence of a master curve. We attribute this embrittlement to limited transmission of tension along polymer chains at the crack tip due to solvent viscosity, which reduces the fraction of load-bearing chain segments at rupture. In contrast, in short-chain networks, the tension can readily be transmitted to the entire polymer chains, resulting in a non-negative slope. At sufficiently high viscosity and velocity, energy dissipation by viscosity dominates the tension transmission, resulting in a positive slope regardless of the chain length. These results advance the understanding of toughness dynamics through tension transmission and viscous dissipation.

View Article Online
DOI: 10.1039/D6SM00297H

1. Introduction

The crack propagation in solids can be described through free energy.[1] Consider two solids with different crack areas, being stretched at a fixed displacement. The difference in Helmholtz free energy (F) between the solids per unit area of the crack plane (A) consists of two major terms: a reduction in elastic energy due to the geometric difference and an increase in free energy due to the fracture near the crack tip. The former is called energy release rate G, and the latter is called fracture energy Γ, or toughness: $\mathrm{d}F(A)/\mathrm{d}A = -G + \Gamma$. The competition of two terms predicts the onset of crack propagation. For example, when $G > \Gamma$, the free energy decreases as the crack area increases, thereby advancing the crack. In brittle solids, the fracture process near the crack tip merely includes surface generation, so the toughness is comparable to the surface energy.[2] In tough solids, by contrast, the fracture process involves various mechanisms that increase the free energy, such as chemical/physical bond breaking, friction, and dislocation processes, followed by irreversible thermal dissipation into the environment. Such energy dissipation by crack propagation is often far greater than surface energy, determining the toughness.[3]

In polymer networks, such as gels and elastomers, energy dissipation is often attributed to interchain friction, as captured by viscoelasticity.[4–6] Gent and Petrich have experimentally demonstrated the effects of viscoelasticity on toughness using uncrosslinked rubbers in a peeling test, providing insights into the mechanical behavior of crosslinked rubbers at relatively high peeling velocities.[7] When a strip of uncrosslinked rubber is peeled at different temperatures and velocities, the peeling force as a function of velocity shows a master curve after time-temperature superposition, indicating that the behavior originates from viscoelasticity.[8] The master curve exhibits a nonmonotonic behavior: an increase in the liquid regime, a sudden drop at the liquid-rubbery transition, an increase in the rubbery regime, and a decrease at the rubbery-glassy transition.[9] The failure mode was a cohesive failure at positive slopes, meaning that the peeling force measures the toughness. This observation shows that toughness increases by enhancing energy dissipation arising from viscoelasticity.[9,10] Such viscous energy dissipation has long been used to explain fracture behavior in polymer networks. For example, viscoelastic polymer networks exhibit high hysteresis, and the toughness increases with hysteresis.[11–14] The viscoelasticity depends on the type of polymer chains and is regarded as a material property.

In gels, by contrast, interchain friction can also be easily controlled by using the solvent with different viscosities. Physical gels swollen with glycerol of different concentrations show that toughness increases with solvent viscosity.[15] Siavoshani et al. demonstrate that hydrogels exhibit increased strength and toughness when the solvent is exchanged from water to concentrated glycerol solution, which is attributed to the prolonged bond and network lifetimes in the more viscous solvent.[16]

The effects of solvent viscosity can be indirectly studied by varying the stretch rate, assuming that the shear due to viscosity scales with the far-field stretch rate. Hassan et al. show that long-chain polyacrylamide (PAAm) single-network hydrogels exhibit near-perfect elasticity with negligible hysteresis in the absence of a crack, whereas the fracture properties with a crack, such as toughness, decrease as the stretch rate increases.[17,18] This reversed relation between toughness and stretch rate can be attributed to the shear-lag effect: the solvent and the polymer chain are subject to high relative motion at the crack tip, where the shear limits the diffusion of tension along

View Article Online
DOI: 10.1039/D6SM00297H

the polymer chain. The shear-lag model predicts a characteristic length that bears a tension, referred to as the slip zone l_b, which scales with the polymer-chain modulus, solvent viscosity, and local strain rate.[17,19] Thus, l_b exhibits rate dependence due to viscosity and strain rate that introduce a time scale. Meanwhile, the Lake–Thomas model predicts that the fracture energy of polymer networks scales with the number of monomers that bear a tension ahead of the crack tip.[12] Together, these models establish a scaling framework that captures the toughness dynamics of polymer networks. However, direct evidence of how solvent viscosity affects the diffusion of tension along polymer chains, especially in simple single networks, is lacking. Furthermore, it was assumed that the far-field stretch rate applied by the tensile tester is proportional to the local strain rate near the crack tip, so that the dynamics of shear-lag effects at the molecular scale can be experimentally studied by varying the far-field stretch rate. However, although the far-field stretch rate and the local strain rate are expected to be in a positive monotonic relation, it is challenging to experimentally determine their scaling relation due to limited spatiotemporal resolution[20].

Here, we directly investigate how solvent viscosity affects the toughness of long-chain polymer networks. We hypothesize that viscosity determines the diffusion of tension along the polymer chains ahead of a crack tip, thereby affecting the degree of shear-lag and toughness (**Figure 1**). When the viscosity is low, the friction on the polymer chain by the solvent is relatively small. Therefore, the tension on the polymer chain can be transmitted along the entire polymer chain length (**Figure 1A**). When the chain breaks, the elastic energy stored in this polymer chain dissipates, determining the toughness. When the viscosity is high, by contrast, the transmission of tension along the polymer chain will be hindered by high solvent friction (**Figure 1B**). Because the polymer chain ahead of the crack tip is pulled by crosslinked chains, the polymer segments near the crosslinks will be fully stretched, while the segments far from the crosslinks will remain relaxed. Consequently, high viscosity will reduce the portion of the polymer chain under stretch at rupture, lowering the toughness. For short-chain polymer networks, tension can be transmitted along the entire polymer chain regardless of viscosity (**Figure 1C-D**). Therefore, toughness will increase with viscosity due to greater energy dissipation by friction, consistent with the traditional understanding of the relationship between toughness and viscosity.

View Article Online
DOI: 10.1039/D6SM00297H

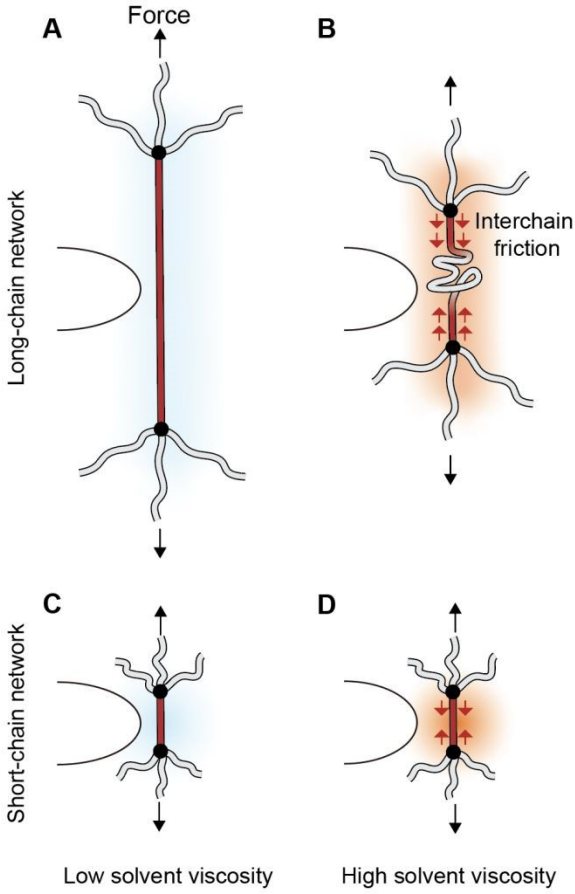

Figure 1. A polymer chain ahead of the crack tip at different viscosities and chain lengths. A. Long chain at low viscosity. **B.** Long chain at high viscosity. **C.** Short chain at low viscosity. **D.** Short chain at high viscosity.

As a model material, we use single-network polyacrylamide (PAAm) gels. We first synthesize identical PAAm hydrogels using water as a solvent (**Figure 2A**). Then, we exchange the solvent from water to glycerol solutions. Depending on the concentration, the viscosity (η) varies from 10^{-3} Pa·s to 10^{0} Pa·s (**Figure 2B**, Table S1).[21] We control the swelling time to fix the polymer content (**Figure 2C**, Table S2). Therefore, the resulting gels have identical polymer network structure and polymer content but significantly different solvent viscosities. Note that both water and glycerol are good solvents for polyacrylamide. The equilibrium swelling ratio of water is about 5.5, and that of glycerol is 6.6. The polymer conformation can differ with glycerol concentration due to differences in polymer-solvent interactions. However, we assume its effects are insignificant, given that our focus is on polymer chain rupture at large deformation. We will also compare long-chain and short-chain networks using the same procedures to investigate their difference in the effects of solvent viscosity. The prepared samples will be subjected to various mechanical tests, including uniaxial tension without a crack and pure shear and trouser tests with a crack, to measure toughness. These experimental data will provide quantitative relationships between viscosity and toughness while holding other aspects of the polymer network constant.

View Article Online
DOI: 10.1039/D6SM00297H

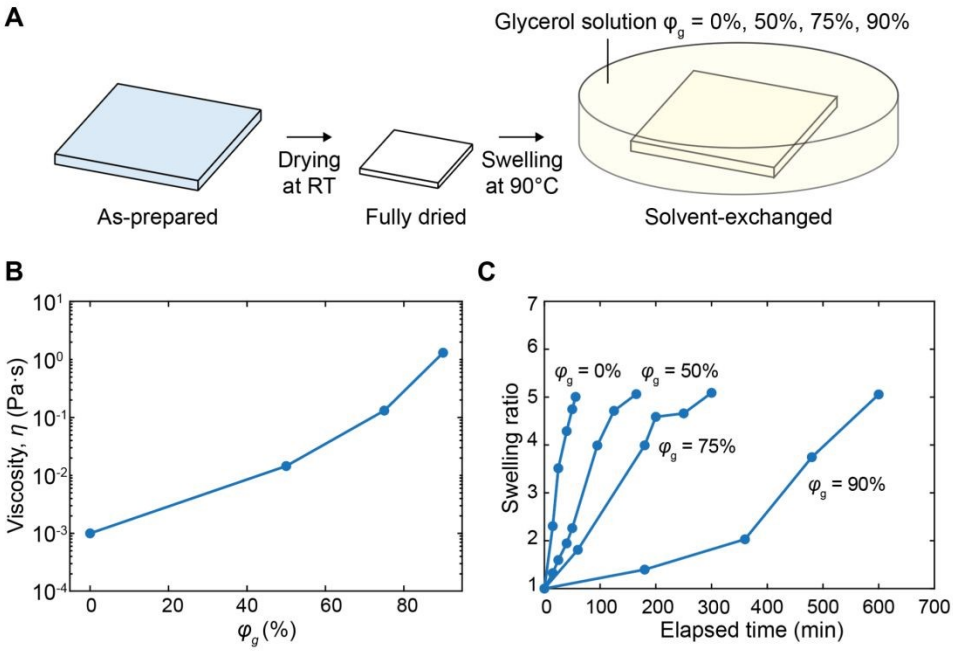

Figure 2. Preparation of PAAm hydrogels with various solvent viscosities. A. Synthesis process. **B**. Viscosity as a function of glycerol concentration φ_g.[21] **C**. Swelling ratio of fully dried hydrogels over time. The samples were swollen until they reached a swelling ratio of 5.

2. Materials and methods

2.1. Preparation of gels with different solvent viscosity

Polyacrylamide gels were synthesized using acrylamide (AAm, A8887, Sigma-Aldrich) as monomer, N,N'-methylenebisacrylamide (MBAA, M7279, Sigma-Aldrich) as crosslinker, 2-hydroxy-4'-(2-hydroxyethoxy)-2-methylpropiophenone (Irgacure 2959, 410896, Sigma-Aldrich) as photoinitiator, and deionized water (DI water) as solvent. A stock monomer solution was prepared by dissolving 30 g of AAm in 15 mL of water. Stock solutions of crosslinker (0.1 M in water) and initiator (0.1 M in ethanol) were also prepared. Precursor solutions were mixed to achieve desired water-to-monomer (*W*), crosslinker-to-monomer (*C*), and initiator-to-monomer (*I*) ratios, with *I*/*C* fixed at 0.4. Long-chain gels were prepared with $C = 10^{-5}$, whereas short-chain gels were prepared with $C = 10^{-3}$. For high *C* conditions, the crosslinker and initiator were used directly without dilution. All precursor solutions were degassed by ultrasonication for 5 min at room temperature. Molds were assembled from glass plates (8476K15, McMaster-Carr) and rubber spacers (1460N21, McMaster-Carr), sealed with binder clips, and filled with precursor solution. The precursor was cured under ultraviolet irradiation (Sankyo Denki, F8T5BL, 1.5 mW cm^{-2}) for 3 hours. After curing, gels were removed from molds, fully dried, and weighed. The fully dried samples were immersed in different solutions at 90°C until the swelling ratio reached 5, ensuring identical polymer content across all samples.

View Article Online
DOI: 10.1039/D6SM00297H

2.2. Rheology test

Cylindrical samples (25 mm in diameter and 1 mm in thickness) were prepared for rheological measurements. The experiments were conducted at 25°C using a rotational parallel-plate rheometer (Anton Paar; MCR 302). A flat plate geometry (PP-25, 25 mm diameter) was employed. To minimize slippage between the samples and the plates, a normal force of approximately 7 N was applied prior to the measurement. The storage modulus (G') and loss modulus (G") were then recorded as functions of angular frequency.

2.3. Uniaxial tension test

Dogbone-shaped specimens were tested with a tensile tester (Instron; 34TM-30) at a stretch rate of 0.2 s^{-1} over a solvent viscosity range from 10^{-3} to 10^{0} Pa·s, with five samples measured per condition to ensure data reliability. The strength is calculated as the maximum force divided by the cross-sectional area in the reference state. The stretchability is defined as the change in length divided by the initial length in the reference state. Young's modulus is calculated from the initial slope (stretch: 1.04~1.07) of the stress-stretch curves.

2.4. Pure shear test

Toughness was measured using the pure shear test (**Figure 3A**). The sample dimensions were 8 cm × 1 cm × 1 mm. By monotonically stretching the sample without a crack, the elastic energy density $W(\lambda)$ was obtained. The stretch λ was defined by the height of the sample in the stretched state divided by the height of the sample in the reference state. By monotonically stretching the sample with a crack, we measured λ_c, the critical stretch where the crack starts to propagate. The toughness was given as $\Gamma = W(\lambda_c)H_0$ (**Figure 3B**). All experiments were repeated four times to ensure data reliability.

View Article Online
DOI: 10.1039/D6SM00297H

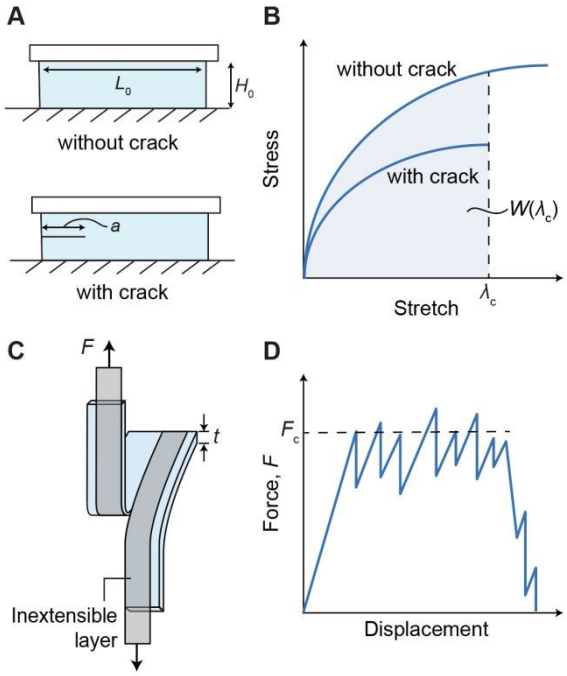

Figure 3. Schematic illustration of the samples to measure the toughness. A. A pure shear sample without a crack (top) and with a crack (bottom). H_0 is the height of the sample at the undeformed state. L_0 is the width of the sample. *a* is the crack length. **B.** Stress-stretch curves of samples with and without a crack. **C.** A long strip sample used for the trouser test. *t* is the thickness of the sample. **D**. Force-displacement data collected from the trouser test.

2.5. Trouser test

In addition to the pure shear test, the toughness was further measured using the trouser test (**Figure 3C**). The inextensible backing layers were attached to the long-strip sample with a pre-cut crack to fully relax the sample after being torn. Also, these layers guide the crack to be straight, confirming the stress field remains unchanged as the crack grows. Each strip was pulled in the opposite direction at a constant velocity *v*, while measuring force *F* (**Figure 3D**). When the crack grows by d*a*, both strips move by d*a*, so the external work is given as $2F_c$d*a*. The area of the crack plane increases by *t*d*a*, where *t* is the thickness of the strip. Thus, the toughness measured by the trouser test is given as $\Gamma = 2F_c/t$, where F_c is the plateau value of the peeling force. When the stick-slip is severe, we collect peak values to calculate toughness.

3. Results

3.1. Homogeneous deformation

The rheological properties of samples of various solvent viscosities (η = 10^{-3}, 10^{-2}, 10^{-1}, and 10^{0} Pa·s) and two chain lengths (C = 10^{-5} and 10^{-3}) are measured (**Figure 4A-B**). To quantitatively compare the effective chain length of the two networks, we estimate the average number of monomers of elastically effective chains (n) from the plateau modulus measured (G'). Assuming an ideal polymer network in which polymer chains are Gaussian chains, n and G' are related as n =

View Article Online
DOI: 10.1039/D6SM00297H

$\varphi kTJ^{2/3}/(G'\Omega)$, where φ is the final polymer volume fraction, Ω is the monomer volume of polyacrylamide, kT is the temperature in joules, and J is the swelling ratio with respect to the as-prepared state.[22] Using $\Omega = 1.05 \times 10^{-28}$ m^3, T = 300K, φ = 20%, and J = 3.3, the measured plateau moduli predict n = 120-175 for $C = 10^{-3}$ and n = 220-440 for $C = 10^{-5}$. At the higher crosslinker concentration ($C = 10^{-3}$), n reflects the chain length between neighboring chemical crosslinkers. In contrast, at the lower crosslinker concentration ($C = 10^{-5}$), the network is highly entangled, so n reflects the chain length between neighboring entanglements. Instead, we estimate it by the scaling relation from the n value at $C = 10^{-5}$: $n \sim C^{-1}$,[23] resulting in n = 12,000-17,500. These two systems are regarded as representative short-chain and long-chain polymer networks, respectively.

Both storage and loss moduli are insensitive to η over a wide range of angular frequency. The moduli at $C = 10^{-3}$ are higher than those at $C = 10^{-5}$ at all viscosities, indicating that the modulus is determined by the network structure and the contribution of viscosity is relatively small. All samples exhibit a high level of elasticity with orders of magnitude difference between G' and G'', suggesting that the friction by solvent viscosity is relatively small. We also measure the stress-stretch curves under uniaxial tension (**Figure 4C**). The modulus is insensitive to η but sensitive to C, as we can observe in the rheology data (**Figure 4D**, Table S3). We attribute this observation to homogeneous deformation in the absence of a crack tip, where the relative motion between polymer chains and solvent is minimal and the effects of viscosity are negligible. However, the fracture properties at $C = 10^{-5}$ are sensitive to η. The curves at $C = 10^{-3}$ mostly overlap as η varies, while the curves at $C = 10^{-5}$ only overlap at a small deformation with different fracture points. The strength and stretchability exhibit negative correlation with η at $C = 10^{-5}$, whereas no clear correlation is observed at $C = 10^{-3}$ (**Figure 4E-F**, Table S4-5). This negative correlation in long-chain polymer networks contrasts to the positive correlation of the existing understanding that solvent viscosity strengthens the polymer networks.[16] However, a molecular-level interpretation of this trend remains limited because mechanistic theories describing fracture properties without a crack are lacking.

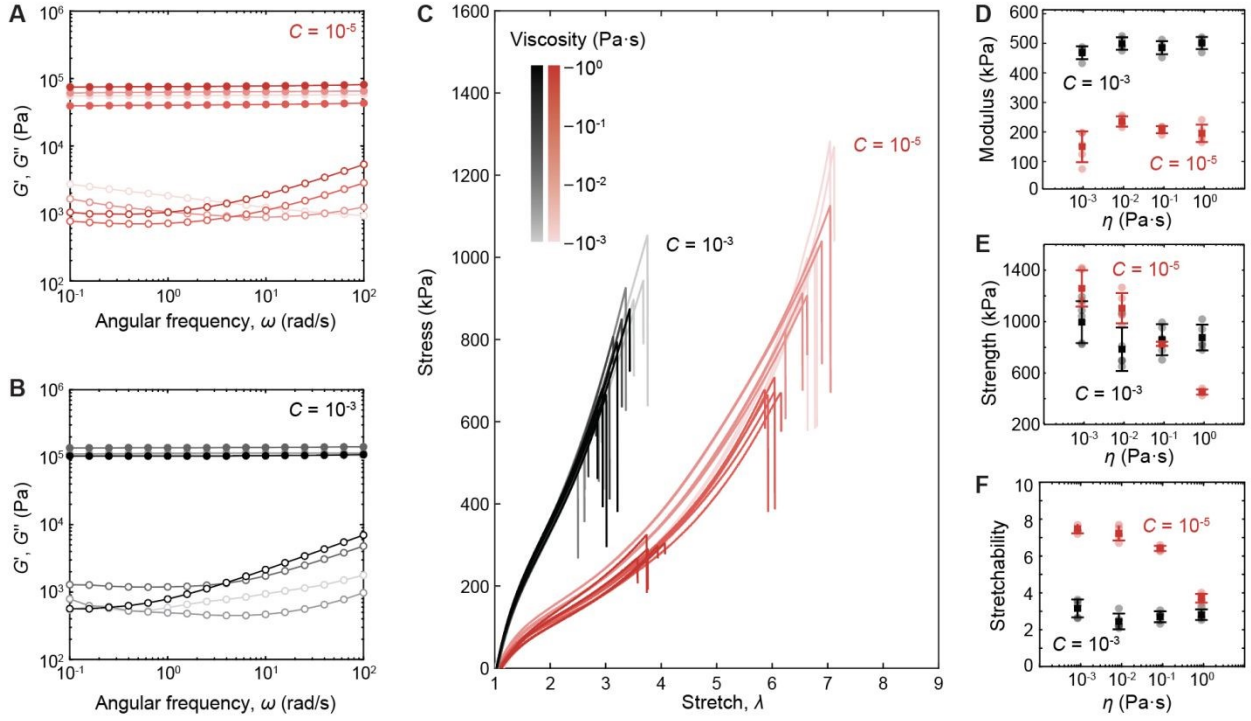

View Article Online
DOI: 10.1039/D6SM00297H

Figure 4. Mechanical properties without a crack. Rheological properties of samples with various solvent viscosities η at **A.** $C = 10^{-5}$ and **B**. $C = 10^{-3}$. **C.** Stress-stretch curves of samples with various values of η and two values of C. **D.** Modulus, **E.** strength, and **F.** stretchability as a function of η at two values of C.

3.2. Toughness with pure shear test

We use the pure shear test to measure the fracture toughness of gels (**Figure 5**, Table S6). In this geometry, where the width is much greater than the height and the crack length, the energy release rate is nearly constant as the crack propagates. The energy release rate is a monotonically increasing function of far-field stretch. At the critical stretch, the corresponding energy release rate reaches the toughness regardless of crack length, leading to catastrophic fracture. The crack velocity, which is directly related to the local strain rate at the crack tip and the shear-lag model, is close to the shear wave velocity[24], and is not imposed by the test. Instead, the test imposes the far-field stretch rate, which is indirectly related to the local strain rate only at the initiation of crack propagation, and even their scaling relation remains unclear. Despite these limitations, pure-shear tests on samples with various solvent viscosities will provide an experimental scaling relation for the rate dependence of initiation of crack propagation, offering partial experimental evidence for the shear-lag effect.

At $C = 10^{-5}$, toughness decreases significantly as η increases. At low viscosity (10^{-3} Pa·s), the toughness reaches ~2,000 J/m^2, but it drops to ~400 J/m^2 in intermediate viscosity solvents. We observe that the toughness scales with $\eta^{-1/4}$ for 10^{-3} Pa·s < η < 10^{-1} Pa·s with the coefficient of determination of 0.78. We attribute this scaling relation to the shear-lag effects. Let l_b be the length scale of the polymer chain under tension, and consider a polymer chain ahead of the crack tip as a rigid fiber under shear. The shear-lag model predicts $l_b \sim \eta^{-1/2}$, and the Lake-Thomas model predicts the toughness $\Gamma \sim l_b^{1/2}$.[12] Thus, $\Gamma \sim \eta^{-1/4}$.[17,19] This scaling relation suggests that, at the viscosities used in this study, the polymer chain ahead of the crack tip is not fully stretched at rupture due to the shear-lag effect. As η increases, the portion of the fully stretched polymer chain decreases, embrittling the polymer network.

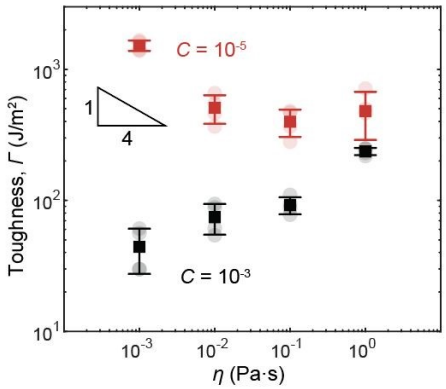

Figure 5. The toughness Γ of the long-chain gels and the short-chain gels as a function of solvent viscosity η.

View Article Online
DOI: 10.1039/D6SM00297H

At the highest viscosity (10^0 Pa·s), however, the toughness deviates from the scaling relation and increases to ~500 J/m^2. This observation indicates that the energy dissipation due to the viscosity dominates the diffusion of tension in polymer chains. This positive correlation between toughness and viscosity is observed in all viscosities used in this study at C = 10^{-3}. The polymer chain is expected to be 100 times shorter than the samples with C = 10^{-5}, so the tension can readily be transmitted to the entire polymer chain. Therefore, the higher viscosity simply increases the toughness as an additional source of energy dissipation. In addition, at this high viscosity, the toughness values at C = 10^{-3} and C = 10^{-5} increase with a similar slope, corroborating our interpretation.

3.3. Toughness with trouser test

We also use the trouser test to measure the fracture toughness of gels. To simplify the analysis, we attach inextensible yet sufficiently flexible backing layers to the specimen. This backing layer fully relaxes the specimen underneath after being torn, so the stress field around the crack tip simply shifts as the crack propagates. For the flexibility of the specimen and backing layer, we neglect the bending energy. Therefore, at steady-state crack propagation, the toughness is the external work per unit crack area, given by $2F_c/t$. The factor of 2 arises from the fact that the crack velocity is half of the pulling velocity (v) set by the tensile tester. One of the differences between the pure shear test and the trouser test is that the trouser test imposes the crack velocity that determines the deformation rate near the crack tip. Therefore, trouser tests enable direct investigation of shear-lag effects by controlling both the local strain rate with the pulling velocity, as well as the solvent viscosity.

We prepare samples with 4 viscosities and 2 chain lengths, apply 5 velocities, and measure the peeling force as a function of displacement. At C = 10^{-5}, a significant stick-slip occurs under low viscosity and low velocity, suggesting that toughness and velocity are in a negative correlation (**Figure 6A**).[7] As the velocity and viscosity increase, the stick-slip disappears and exhibits a stable plateau. At C = 10^{-3}, by contrast, most conditions show a stable plateau with moderate stick-slip, suggesting a positive correlation between toughness and velocity (**Figure 6B**). Also, the toughness values are lower than those at C = 10^{-5} overall (note that the vertical scale bars for the C = 10^{-5} and C = 10^{-3} panels differ by a factor of 5).

View Article Online
DOI: 10.1039/D6SM00297H

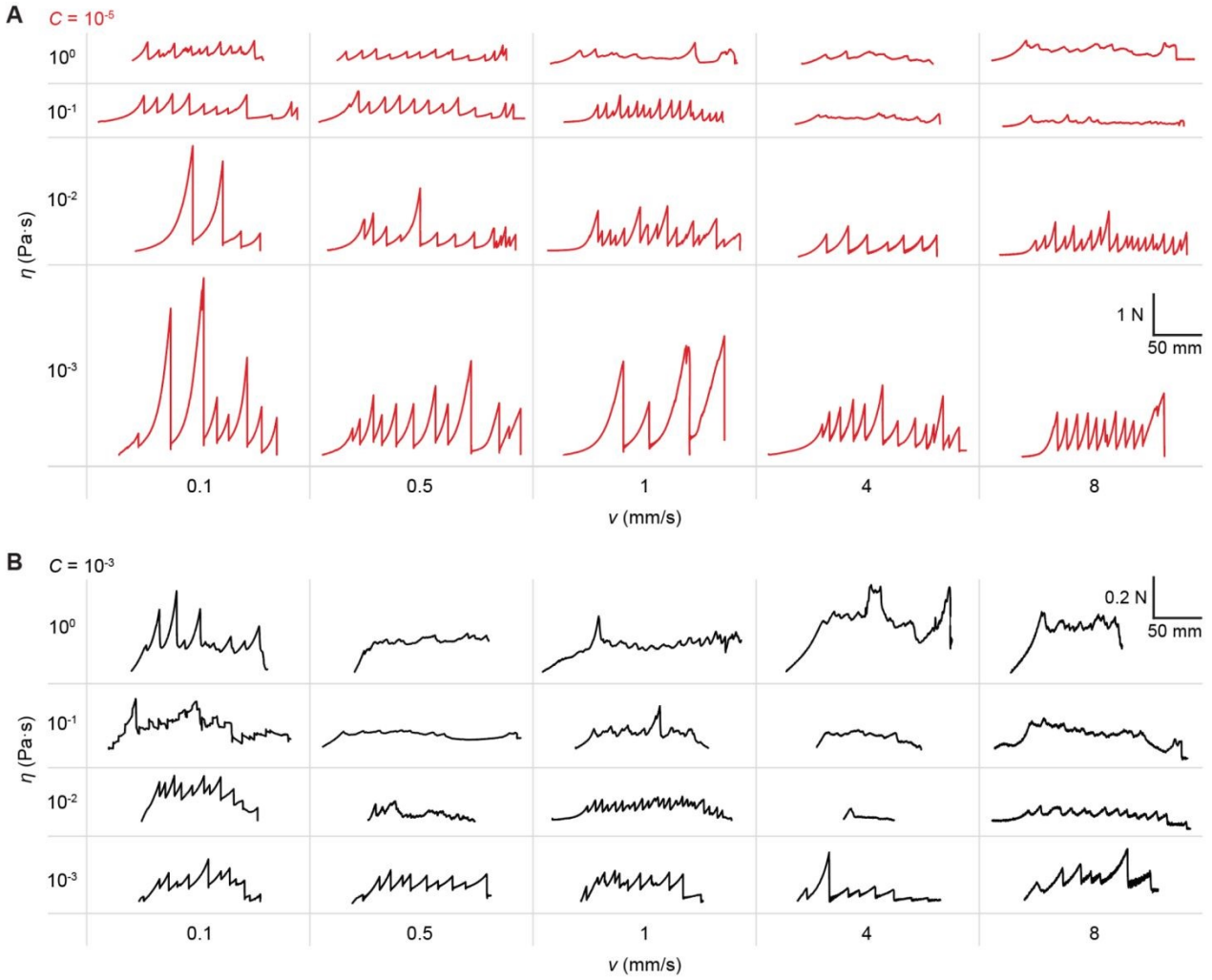

Figure 6. Force as a function of displacement in the trouser test for samples of various viscosities η at pulling velocities v. **A.** At $C = 10^{-5}$. The scale bar is 1 N in height and 50 mm in width. **B.** At $C = 10^{-3}$. The scale bar is 0.2 N in height and 50 mm in width.

We plot the measured toughness Γ as a function of viscosity η (**Figure 7A**, Table S7). At both C values, the correlation between Γ and η is unclear due to large scatter. In addition, at $C = 10^{-5}$, higher v gives lower Γ at $\eta = 10^{-1}$ Pa·s, whereas such a trend is not evident at other viscosities. The coefficient of determination to $\Gamma \sim \eta^{-1/4}$ is 0.56, which is relatively low. Overall, the data do not reveal a clear trend. Incidentally, in the shear-lag model, not only v (mm/s) but also η (Pa·s) has a time scale. Considering that these are the only variables that introduce a time scale into the model, ηv (Pa·m) will fully determine the dynamics of toughness. Specifically, the shear-lag model predicts $l_b \sim (\eta v)^{-1/2}$, so the Lake-Thomas model predicts $\Gamma \sim l_b^{1/2} \sim (\eta v)^{-1/4}$. To test this scaling relation, we plot Γ as a function of ηv (**Figure 7B**). For $C = 10^{-5}$, the toughness generally decreases with increasing ηv, following the scaling relation $\Gamma \sim (\eta v)^{-1/4}$ with a higher coefficient of determination of 0.77. At high ηv, the energy dissipation by viscosity dominates, increasing the toughness. By contrast, at $C = 10^{-}$

View Article Online
DOI: 10.1039/D6SM00297H

^{3} and modest ηv, toughness is nearly constant with respect to ηv. We attribute this to the fact that the polymer chains are sufficiently short to be fully stretched at a wide range of ηv. At high ηv, the toughness increases with ηv, possibly due to the viscous energy dissipation, similar to the case of $C = 10^{-5}$.

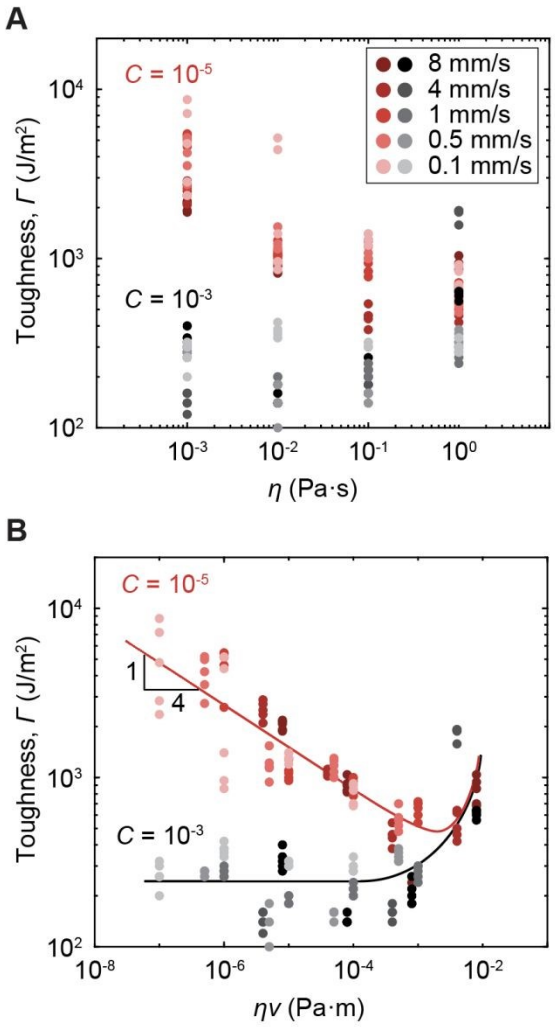

Figure 7. The toughness Γ of the long-chain gels and the short-chain gels **A.** as a function of solvent viscosity η, and **B.** as a function of ηv, where v is the pulling velocity.

The stick-slip criteria–the slope of toughness in v–can also be extended to the slope of toughness in ηv. When the master curve exhibits a negative slope, pronounced stick-slip behavior is observed, and the force often relaxes to near zero. When the master curve has a positive slope, the stick-slip behavior is marginal with a stable plateau. When the master curve is flat, the stick-slip behavior is observed, but the force partially relaxes. This observation can be interpreted as follows. Consider a crack propagation in the trouser test at a given ηv when the slope is positive. The crack cannot propagate faster than $v/2$, as a higher ηv requires more energy to dissipate. The crack also cannot propagate slower than $v/2$, as lower ηv accumulates excessive energy and accelerates crack growth. Consequently, the crack grows stably at $v/2$. By contrast, when the slope is negative, the

View Article Online
DOI: 10.1039/D6SM00297H

crack can propagate faster than $v/2$ as higher ηv accumulates excessive energy due to reduced toughness, accelerating the crack propagation (slip). This catastrophic crack propagation temporarily relaxes the specimen and reduces the energy release rate. At $C = 10^{-5}$, the toughness at high ηv (~10^{-3} Pa·m) is ten times lower than that at low ηv (~10^{-7} Pa·m) (**Figure 7B**), consistent with significant slip and relaxation in the force-displacement curve (**Figure 6**). After the slip, the energy release rate continues to increase without crack propagation (stick) as being consistently pulled. The crack slips again when the energy release rate reaches the toughness of the corresponding ηv, which is captured by the peak force in the force-displacement curve.

The master curves can be compared with previous reports on toughness as a function of the stretch rate in pure shear tests.[17] In this experiment, the toughness plateaus at low stretch rates and decreases at high stretch rates, which can also be attributed to the shear-lag effect. When the stretch rate is low, the tension is transmitted throughout the polymer chain, so toughness is limited by chain length. As the stretch rate increases, the shear-lag effect reduces l_b, decreasing the toughness. Therefore, we anticipate that the left limit of the master curve is a plateau that scales with chain length$^{1/2}$, as predicted by the Lake-Thomas model (**Figure 8**). When ηv is excessively high, the polymer chains behave like glassy polymers, reducing toughness.[7]

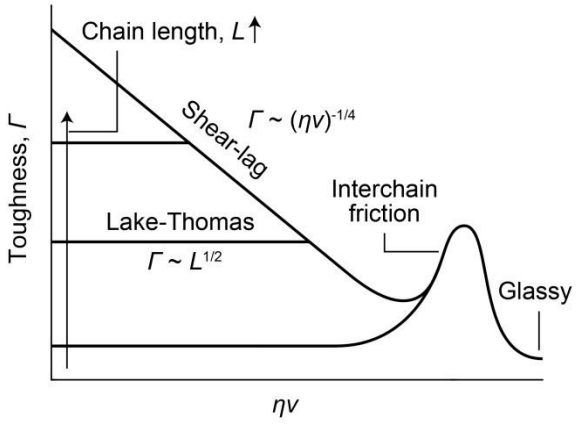

Figure 8. Schematic of toughness dynamics of single polymer networks.

4. Conclusion

We hypothesized that solvent viscosity governs the transmission of tension along polymer chains and thus controls toughness. Our results support this hypothesis and are explained by the shear-lag model. In long-chain gels, a viscous solvent increases the sliding stress between polymer chains and the solvent matrix, shortening the effective shear-lag length and confining tension near the chain ends, reducing toughness. In short-chain gels, where elastic energy is inherently limited, higher solvent viscosity enhances interchain friction during chain pullout, leading to greater toughness. These findings reveal that interchain friction governed by solvent viscosity hinders the transmission of tension through polymer chains, providing a molecular framework for tuning the fracture properties of soft materials.

Our work investigates the toughness dynamics of single polymer networks at a certain range of solvent viscosity and velocity. To extend the understanding of toughness dynamics, one can further consider other types of time-dependency: the transition from uncrosslinked polymers to polymer

View Article Online
DOI: 10.1039/D6SM00297H

networks,[7] the chain bond lifetime that can cause delayed fracture at excessively low ηv,[16,20] poroelasticity,[25] the dynamics of entanglements,[26] crack tip profile,[27] super-shear crack propagation,[24] and the limitations and non-idealities in polymer synthesis.[28]

Author contributions

Haeji Kim: data curation, formal analysis, writing – drafting, reviewing, and editing. Diogo Costa: data curation. Junsoo Kim: supervision, conceptualization, methodology, formal analysis, writing – drafting, reviewing, and editing.

Acknowledgement

This work was primarily supported by the National Science Foundation's MRSEC program (DMR-2308691) at the Materials Research Center of Northwestern University. This work was also supported by start-up funds from Northwestern University.

Conflicts of interest

There are no conflicts of interest to declare.

References

1 T. Kang, J. Dai, Y. Huang, H. Kim, S. Keten and J. Kim, *Chem. Rev.*, 2025, **125**, 11032–11057.
2 A. A. Griffith, *Philos. Trans. R. Soc. Lond. Ser. Contain. Pap. Math. Phys. Character*, 1921, **221**, 163–198.
3 X. Zhao, *Proc. Natl. Acad. Sci.*, 2017, **114**, 8138–8140.
4 K. Tsunoda, J. J. C. Busfield, C. K. L. Davies and A. G. Thomas, *J. Mater. Sci.*, 2000, **35**, 5187–5198.
5 C. Creton and M. Ciccotti, *Rep. Prog. Phys.*, 2016, **79**, 046601.
6 R. Long and C.-Y. Hui, *Soft Matter*, 2016, **12**, 8069–8086.
7 A. N. Gent and R. P. Petrich, *Proc. R. Soc. Lond. Ser. Math. Phys. Sci.*, **310**, 433–448.
8 M. L. Williams, R. F. Landel and J. D. Ferry, *J. Am. Chem. Soc.*, 1955, **77**, 3701–3707.
9 R. S. Rivlin and A. G. Thomas, *J. Polym. Sci.*, 1953, **10**, 291–318.
10 Y. Fukahori, K. Sakulkaew and J. J. C. Busfield, *Polymer*, 2013, **54**, 1905–1915.
11 Z. Wang, C. Xiang, X. Yao, P. Le Floch, J. Mendez and Z. Suo, *Proc. Natl. Acad. Sci.*, 2019, **116**, 5967–5972.
12 G. J. Lake and A. G. Thomas, *Proc. R. Soc. Lond. Ser. Math. Phys. Sci.*, 1967, **300**, 108–119.
13 T. Baumberger and O. Ronsin, *J. Chem. Phys.*, 2009, **130**, 061102.
14 S. Lin, C. D. Londono, D. Zheng and X. Zhao, *Soft Matter*, 2022, **18**, 5742–5749.
15 T. Baumberger, C. Caroli and D. Martina, *Nat. Mater.*, 2006, **5**, 552–555.
16 A. Y. Siavoshani, Z. Fan, M. Yang, S. Liu, M.-C. Wang, J. Liu, W. Xu, J. Wang, S. Lin and S.-Q. Wang, *Soft Matter*, 2024, **20**, 7657–7667.
17 S. Hassan, J. Kim and Z. Suo, *J. Mech. Phys. Solids*, 2022, **158**, 104675.
18 C. H. Ahn, Z. Chen, X. Bao and Z. Suo, *Soft Matter*, 2025, 10.1039.D4SM01521E.
19 S. R. Lavoie, S. Hassan, J. Kim, T. Yin and Z. Suo, *Extreme Mech. Lett.*, 2021, **46**, 101317.
20 S.-Q. Wang, Z. Fan, C. Gupta, A. Siavoshani and T. Smith, *Macromolecules*, 2024, **57**, 3875–3900.
21 J. A. Trejo González, M. P. Longinotti and H. R. Corti, *J. Chem. Eng. Data*, 2011, **56**, 1397–1406.
22 M. Rubinstein and R. H. Colby, *Polymer Physics*, Oxford University Press, 2003.
23 J. Kim, G. Zhang, M. Shi and Z. Suo, *Science*, 2021, **374**, 212–216.

View Article Online
DOI: 10.1039/D6SM00297H

24 M. Wang, S. Shi and J. Fineberg, *Science*, 2023, **381**, 415–419.
25 S. Cai, Y. Hu, X. Zhao and Z. Suo, *J. Appl. Phys.*, 2010, **108**, 113514.
26 S.-Q. Wang, S. Ravindranath, Y. Wang and P. Boukany, *J. Chem. Phys.*, 2007, **127**, 064903.
27 F. Luo, T. L. Sun, T. Nakajima, T. Kurokawa, Y. Zhao, A. B. Ihsan, H. L. Guo, X. F. Li and J. P. Gong, *Macromolecules*, 2014, **47**, 6037–6046.
28 S. P. Danielsen, H. K. Beech, S. Wang, B. M. El-Zaatari, X. Wang, L. Sapir, T. Ouchi, Z. Wang, P. N. Johnson, Y. Hu, D. J. Lundberg, G. Stoychev, S. L. Craig, J. A. Johnson, J. A. Kalow, B. D. Olsen and M. Rubinstein, *Chem. Rev.*, 2021, **121**, 5042–5092.

View Article Online
DOI: 10.1039/D6SM00297H

Data availability

Raw data of Figure 2B-C, 4D-F, 5, and 7A are included in the Supplementary Information.